

Preparation, structure and properties of Fe-based bulk metallic glasses

R. Nowosielski, R. Babilas*

Division of Nanocrystalline and Functional Materials and Sustainable Pro-ecological Technologies, Institute of Engineering Materials and Biomaterials, Silesian University of Technology, ul. Konarskiego 18a, 44-100 Gliwice, Poland

* Corresponding author: E-mail address: rafal.babilas@polsl.pl

Received 11.03.2010; published in revised form 01.06.2010

Materials

ABSTRACT

Purpose: The work presents preparation methods, structure characterization and chosen properties analysis of Fe-based bulk metallic glasses in as-cast state.

Design/methodology/approach: The studies were performed on $\text{Fe}_{43}\text{Co}_{14}\text{Ni}_{14}\text{B}_{20}\text{Si}_5\text{Nb}_4$ metallic glass in form of rings, plates and rods. The amorphous structure of tested samples was examined by X-ray diffraction (XRD), transmission electron microscopy (TEM) and scanning electron microscopy (SEM) methods. The thermal properties of the glassy samples was measured using differential scanning calorimetry (DSC). The soft magnetic properties examination of tested material contained coercive force, initial magnetic permeability and magnetic permeability relaxation measurements.

Findings: The XRD and TEM investigations revealed that the studied as-cast samples were amorphous. Broad diffraction halo is typical for metallic amorphous structures that have a large degree of short-range order. The characteristics of the fractured surfaces showed different zones, which might correspond with different amorphous structures of studied materials. The temperature interval of the supercooled liquid region (ΔT_x) defined by the difference between T_g and T_x , is as large as 56 K for the rod with diameter of 3 mm. Differences in coercivity and magnetic permeability between samples with different thickness might be resulted by some difference of amorphous structure.

Practical implications: The centrifugal casting method and the pressure die casting method are useful to produce bulk amorphous materials in form of rings, plates and rods.

Originality/value: The preparation of studied Fe-based bulk metallic glass in form of rings, plates and rods is important for the future progress in research and practical application of that glassy materials.

Keywords: Amorphous materials; Bulk metallic glasses; Glass-forming ability; Thermal and magnetic properties

Reference to this paper should be given in the following way:

R. Nowosielski, R. Babilas, Preparation, structure and properties of Fe-based bulk metallic glasses, Journal of Achievements in Materials and Manufacturing Engineering 40/2 (2010) 123-130.

1. Introduction

Since amorphous materials were prepared in the Au-Si system alloy in 1960 many scientific investigations have been done. These facts have been informed that amorphous alloys have new atomic configurations, which differ from crystalline alloys [1].

Structural features of amorphous materials have determined many characteristics such as good mechanical properties, useful magnetic properties and unique chemical properties, which have not been achieved from crystalline materials [2].

Based on these results, scientists have concentrated on preparation of metallic glasses, which are special group of amorphous materials. Iron-based metallic glasses have

increased the scientific and engineering importance, because of their good soft magnetic properties, such as low coercive force, high magnetic induction and magnetic permeability [3].

It is important to know that preparation of conventional glassy alloys requires high critical cooling rates of about 10^6 K/s (Fig. 1). Critical cooling rate is necessary to determine a glass-forming ability (GFA) and to produce metallic glasses [2].

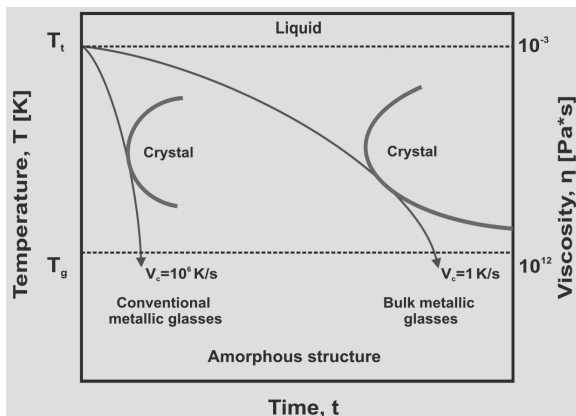


Fig. 1. A comparison of critical cooling rate for conventional and bulk metallic glasses [4]

Scientific investigations of rapid solidification and glass-forming ability processes have succeeded in finding new multicomponent metallic glasses with much lower critical cooling rate. Inoue et al. succeeded in casting Fe-based bulk metallic glasses in Fe-based alloy systems with low critical cooling rates below 10^3 K/s [2,5].

Inoue et al. based on the multicomponents of glassy alloys with high GFA have proposed empirical rules for achieving high glass-forming ability, low critical cooling rate and maximum amorphous sample thickness (Fig. 2). These rules have informed that multicomponent alloy should consist of more than three elements; the alloy should contain two or more metallic elements with different atomic sizes; the metallic elements should have large negative heats of mixing with the metalloid type of components and the alloy should be eutectic [1,2,4].

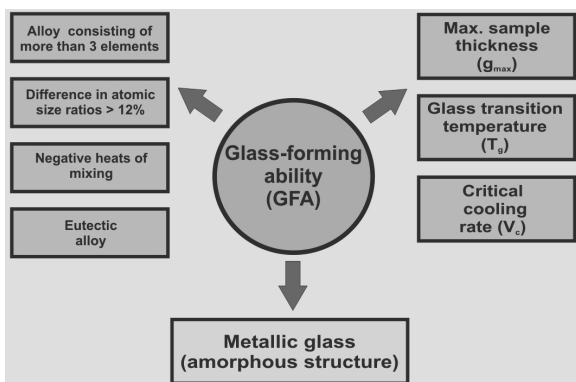


Fig. 2. Schematic correlation between high glass-forming ability, glass transition temperature, maximum sample thickness and critical cooling rate of metallic glasses [1]

2. Material and research methodology

The aim of the paper is the characterization of preparation methods, microstructure, thermal and magnetic properties analysis of Fe-Co-Ni-B-Si-Nb bulk metallic glass in as-cast state. Investigations were done with use of XRD, TEM, SEM, DSC and magnetic measurements methods.

Mixture of pure elements with the nominal composition of $\text{Fe}_{43}\text{Co}_{14}\text{Ni}_{14}\text{B}_{20}\text{Si}_5\text{Nb}_4$ were melted under argon atmosphere to obtain homogeneous ingots. The pre-alloying of the components of studied alloy was carried out by using the ingot preparation equipment presented in Fig. 3. The alloy ingot was prepared in ceramic (Al_2O_3) crucible, which was indirectly heated by graphite crucible by induction coil.

Studied samples were manufactured by the pressure die casting method (plates and rods) and the centrifugal casting method (rings). The pressure die casting technique [6,7] is the method of casting a molten alloy ingot into copper mould under gas pressure. Fig. 4 shows photographic illustrations of the pressure die casting method (including heating and casting stages) used for the production of bulk amorphous plates or rods.

The centrifugal casting method has been used to fabricate the samples of bulk metallic glass in form of rings. This casting method is useful to produce bulk amorphous materials in form of rings, tubes or amorphous matrix composites [8].

The investigated material was cast in form of the ring with diameter of 30 mm and thickness of 0.5 mm, plate with thickness (g) of 1 mm and rod with diameter (ϕ) of 3 mm (Fig. 5).

Structure analysis of the samples in as-cast state was carried out using X-ray diffractometer (XRD) with $\text{Co}_{K\alpha}$ radiation for plate and rod samples examination. The data of diffraction lines were recorded in 2θ range from 35° to 80° .

The fracture morphology of the samples in form of ring, plate and rod was analyzed using the scanning electron microscopy (SEM). Transmission electron microscopy (TEM) was used for the structural characterization of samples in as-cast state. Thin foils for TEM observation (from central part of tested samples) were prepared by an electrolytic polishing method after previous mechanical grinding.

Thermal properties associated with glass transition (T_g), onset (T_x) and peak (T_p) crystallization temperatures and supercooled liquid region (ΔT_x) between T_g and T_x was examined by differential scanning calorimetry (DSC). The heating rate of calorimetry measurements, under an argon protective atmosphere, was 20 K/min.

Magnetic measurements of studied samples in as-cast state, carried at room temperature, included following properties:

- relative magnetic permeability (μ_r) - determined with Maxwell-Wien bridge at a frequency of 1030 Hz and magnetic field $H = 0.5$ A/m [9-11];
- magnetic permeability relaxation ($\Delta\mu/\mu$) also defined as "magnetic after-effects" - determined by measuring changes of magnetic permeability as a function of time after demagnetization, where $\Delta\mu$ is difference between magnetic permeability determined at $t_1 = 30$ s and $t_2 = 1800$ s after demagnetization [12-14];
- coercive force (H_c) - measured by coercivemeter.

Additionally, H_c and $\Delta\mu/\mu$ was determined for samples with different form and thickness.

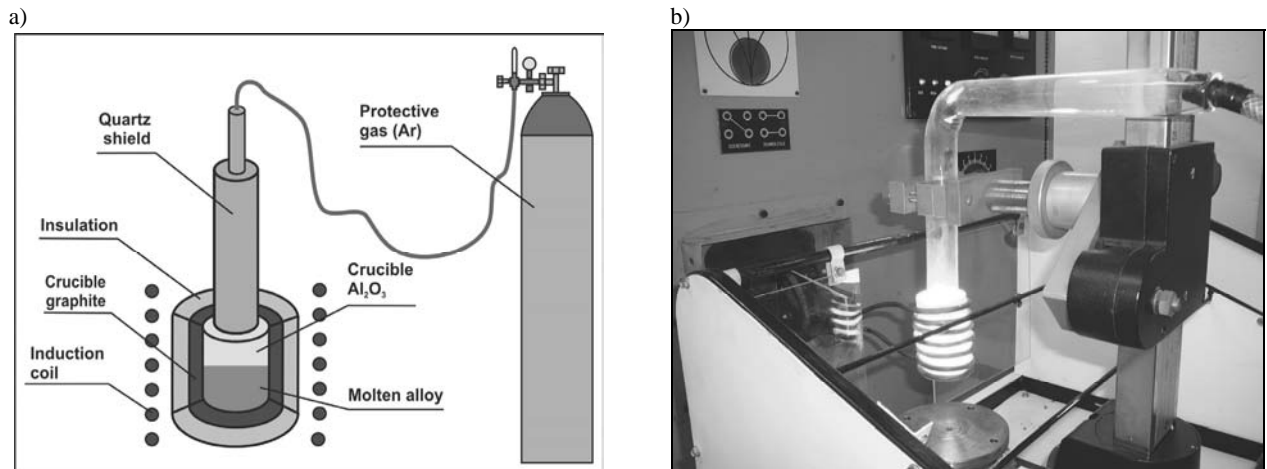


Fig. 3. Preparation of master alloy by induction melting: (a) photograph and (b) schematic illustration of ingot preparation equipment

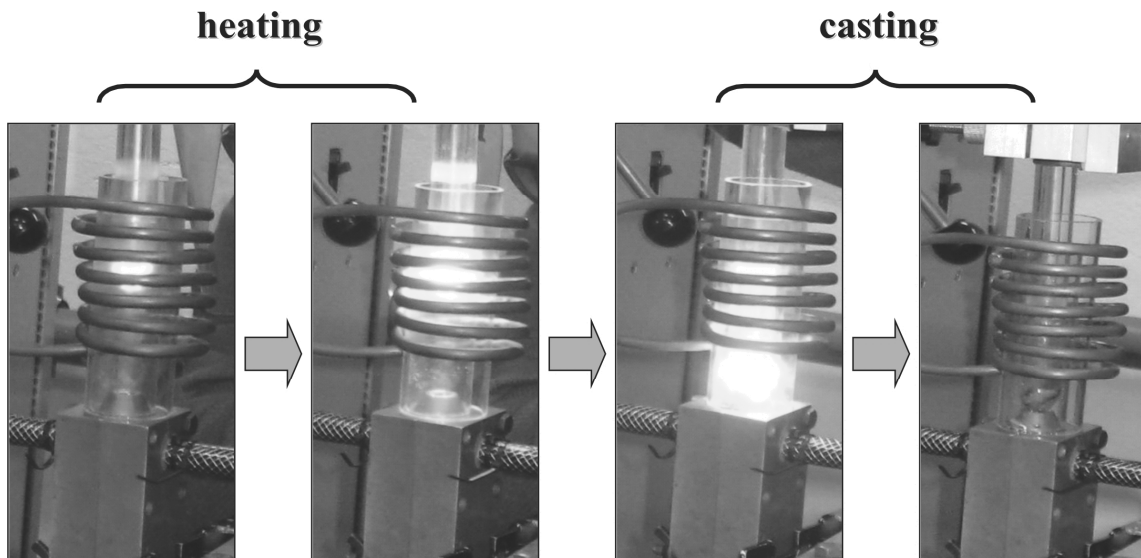


Fig. 4. Chosen stages of the pressure die casting method used for bulk amorphous samples casting



Fig. 5. Outer morphology of cast glassy $\text{Fe}_{43}\text{Co}_{14}\text{Ni}_{14}\text{B}_{20}\text{Si}_5\text{Nb}_4$ alloy samples in form of: a) rings, b) plates, c) rods

3. Results and discussion

The XRD investigations confirmed that the studied as-cast glassy samples were amorphous. The diffraction patterns of tested ring with diameter of 30 mm and thickness of 0.5 mm (Fig. 6a), plate with thickness of 1 mm (Fig. 7a) and rod with diameter of 3 mm (Fig. 8a) show the broad diffraction halo with rounded top

centered at about 52° . This effect is typical of metallic amorphous structures that have a large degree of short-range order.

Figs. 6b, 7b and 8b present TEM images and electron diffraction patterns of the selected samples in as-cast state.

The TEM images revealed only some changes in contrast, which is characteristic for amorphous structure. The electron diffraction patterns consisted only of the halo rings. Broad diffraction halo can be seen for all examined samples.

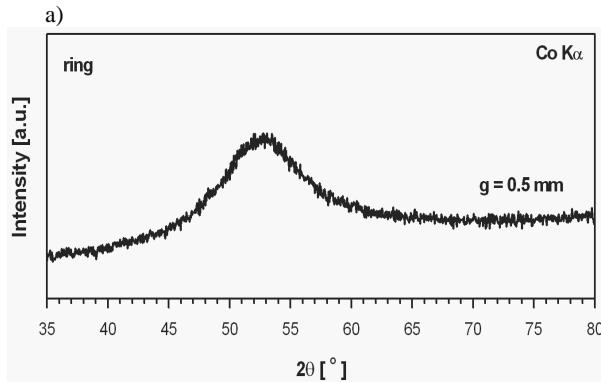


Fig. 6. X-ray diffraction pattern (a) and transmission electron micrograph and electron diffraction pattern (b) of $\text{Fe}_{43}\text{Co}_{14}\text{Ni}_{14}\text{B}_{20}\text{Si}_5\text{Nb}_4$ glassy ring in as-cast state with diameter of 30 mm and thickness of 0.5 mm

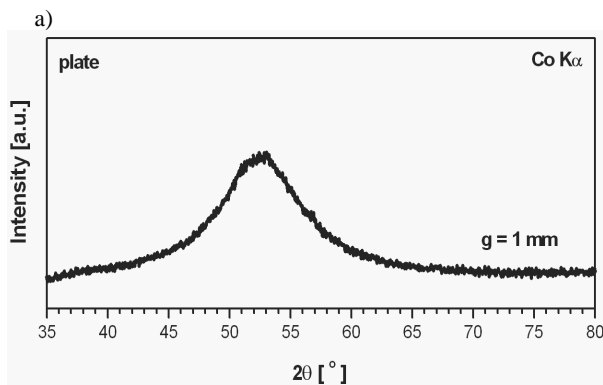


Fig. 7. X-ray diffraction pattern (a) and transmission electron micrograph and electron diffraction pattern (b) of $\text{Fe}_{43}\text{Co}_{14}\text{Ni}_{14}\text{B}_{20}\text{Si}_5\text{Nb}_4$ glassy plate in as-cast state with thickness of 1 mm

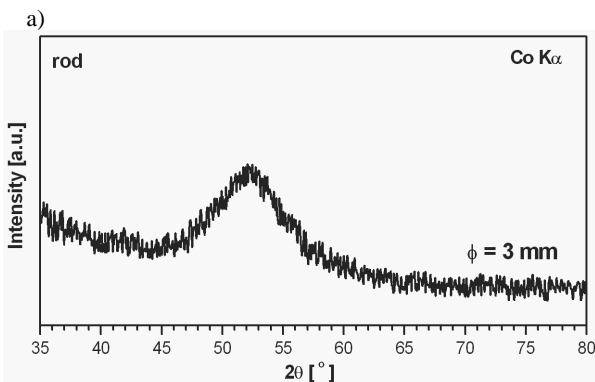


Fig. 8. X-ray diffraction pattern (a) and transmission electron micrograph and electron diffraction pattern (b) of $\text{Fe}_{43}\text{Co}_{14}\text{Ni}_{14}\text{B}_{20}\text{Si}_5\text{Nb}_4$ glassy rod in as-cast state with diameter of 3 mm

These results indicated that tested samples are composed of a single amorphous phase.

Figs. 9-11 show the DSC traces of bulk $\text{Fe}_{43}\text{Co}_{14}\text{Ni}_{14}\text{B}_{20}\text{Si}_5\text{Nb}_4$ alloy at a heating rate of 20 K/min under a flow of argon. The examined alloy prepared in form of ring, plate and rod exhibits the sequence of the glass transition temperature (T_g), onset (T_x) and peak (T_p) crystallization temperature.

The shapes of DSC curves for ring, plate and rod are very similar. The exothermic peaks describing crystallization were observed for all samples. The crystallization effect for the ring sample with diameter of 30 mm and thickness of 0.5 mm includes onset crystallization temperature $T_x = 847$ K and peak crystallization temperature $T_p = 866$ K (Fig. 9).

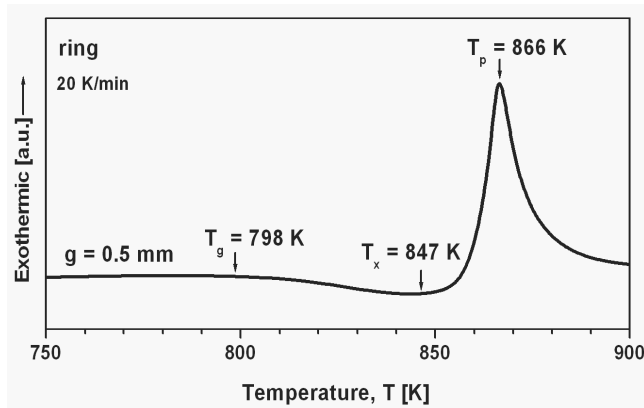


Fig. 9. DSC curves of $\text{Fe}_{43}\text{Co}_{14}\text{Ni}_{14}\text{B}_{20}\text{Si}_5\text{Nb}_4$ glassy alloy ring in as-cast state (heating rate 20 K/min)

In the case of the plate with thickness of 1 mm, the exothermic effect includes onset of the crystallization temperature at $T_x = 849$ K and peak crystallization temperature at $T_p = 872$ K (Fig. 10). For the rod with diameter of 3 mm onset crystallization temperature reached a value of 854 K and peak crystallization temperature was 879 K, respectively (Fig. 11).

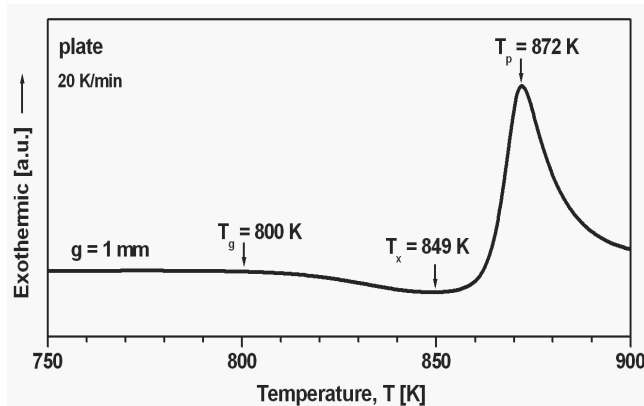


Fig. 10. DSC curves of $\text{Fe}_{43}\text{Co}_{14}\text{Ni}_{14}\text{B}_{20}\text{Si}_5\text{Nb}_4$ glassy alloy plate in as-cast state (heating rate 20 K/min)

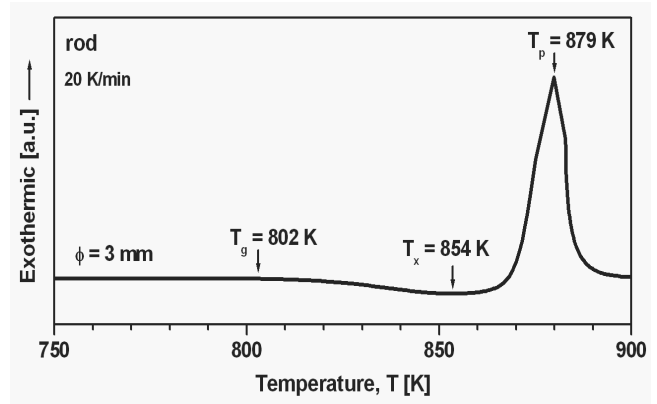


Fig. 11. DSC curves of $\text{Fe}_{43}\text{Co}_{14}\text{Ni}_{14}\text{B}_{20}\text{Si}_5\text{Nb}_4$ glassy alloy rod in as-cast state (heating rate 20 K/min)

The DSC analysis allowed to determine glass transition temperatures of examined glassy samples, which was 798 K for ring, 800 K for plate and 802 K for rod, respectively.

Obtained results of DSC investigations confirmed that the crystallization temperatures: (T_x), (T_p) and glass transition temperature (T_g) increased with increasing of the sample thickness. These results might be due to the changes in the amorphous structure of tested glassy materials.

The temperature interval of the supercooled liquid region (ΔT_x) defined by the difference between T_g and T_x , is as large as 56 K for the rod with diameter of 3 mm, which is very close to 60 K reported by Inoue et al. [15].

The thermal properties parameters of studied glassy samples: glass transition temperature (T_g), onset crystallization temperature (T_x) and supercooled liquid region (ΔT_x) are presented in Table 1.

Table 1.

Thermal properties of the studied $\text{Fe}_{43}\text{Co}_{14}\text{Ni}_{14}\text{B}_{20}\text{Si}_5\text{Nb}_4$ samples in forms of ring, plate and rod, in as-cast state

Sample	Thickness [mm]	T_g [K]	T_x [K]	ΔT_x [K]
ring	0.5	798	847	49
plate	1	800	849	49
rod	3	802	854	56

The fracture surface of the investigated samples in form of ring, plate and rod was investigated by SEM at different magnifications. Figs. 12, 13 and 14 present schematic illustration of tested samples and SEM micrographs of selected areas of examined glassy materials.

The characteristics of the fractured surfaces showed different fracture zones. The fractures could be classified as mixed types with indicated zones contain weakly formed “river” and “shell” patterns (Zone I) and “smooth” areas (Zone II). The schematic illustrations of studied samples also included indicated zones. The fracture surface of two zones probably informed about different amorphous structures of the tested glassy materials.

The coercive force (H_c) of tested metallic glass had a value of 19 A/m for glassy ring with thickness of 0.5 mm. H_c for glassy plate with thickness of 1 mm was 41 A/m. What is more,

the coercive force had a value of 78 A/m for rod with diameter of 3 mm. Fig. 15 presents coercive force versus sample thickness for studied alloy (included samples with different thickness).

However, differences in coercivity between samples with different thickness were observed. These increased values of coercivity might suggest some difference of amorphous structure.

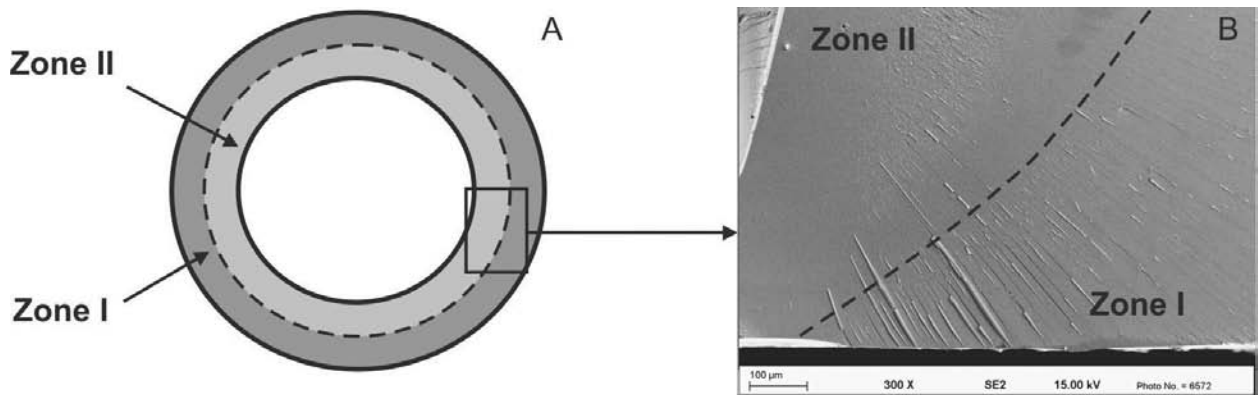


Fig. 12. Fracture morphology of $\text{Fe}_{43}\text{Co}_{14}\text{Ni}_{14}\text{B}_{20}\text{Si}_5\text{Nb}_4$ amorphous ring in as-cast state with diameter of 30 mm and thickness of 0.5 mm: A – schematic illustration of sample, B – SEM micrograph, magn. 300x

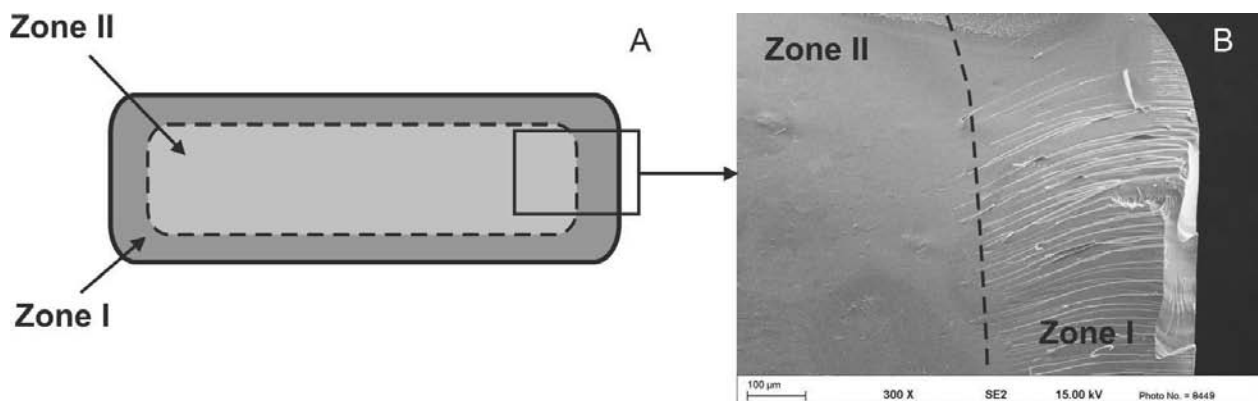


Fig. 13. Fracture morphology of $\text{Fe}_{43}\text{Co}_{14}\text{Ni}_{14}\text{B}_{20}\text{Si}_5\text{Nb}_4$ amorphous plate in as-cast state with thickness of 1 mm: A – schematic illustration of sample, B – SEM micrograph, magn. 300x

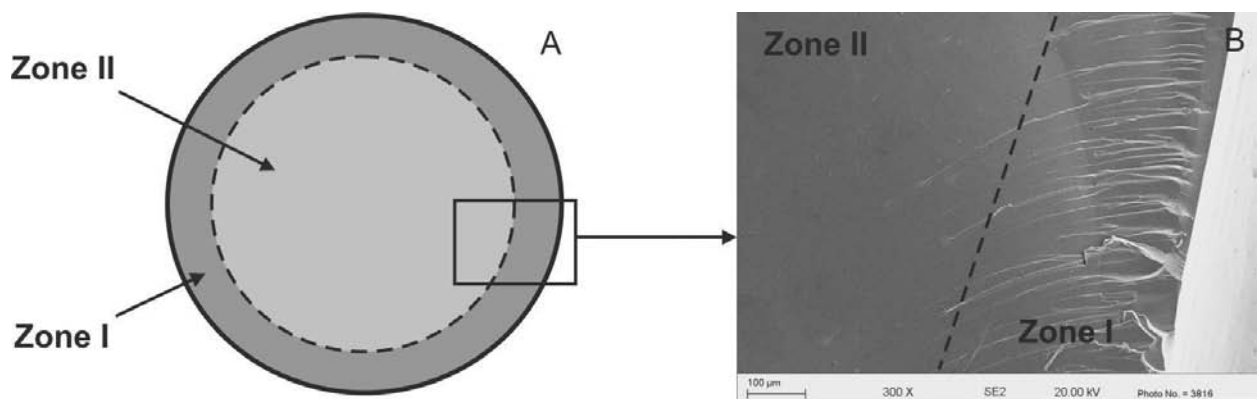


Fig. 14. Fracture morphology of $\text{Fe}_{43}\text{Co}_{14}\text{Ni}_{14}\text{B}_{20}\text{Si}_5\text{Nb}_4$ amorphous rod in as-cast state with diameter of 3 mm: A – schematic illustration of sample, B – SEM micrograph, magn. 300x

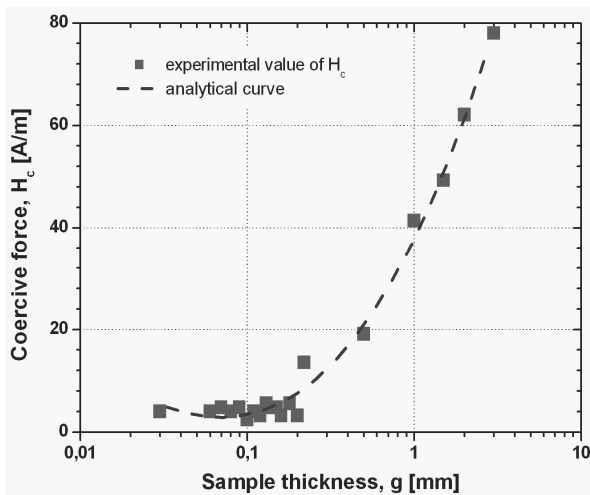


Fig. 15. Coercive force of $\text{Fe}_{43}\text{Co}_{14}\text{Ni}_{14}\text{B}_{20}\text{Si}_5\text{Nb}_4$ alloy versus sample thickness

The initial magnetic permeability (μ_r) was 1006 for ring with thickness of 0.5 mm, $\mu_r = 879$ for plate sample with thickness of 1 mm. Moreover, the initial magnetic permeability of studied ring had a lower value $\mu_r = 147$.

The magnetic permeability relaxation of the tested alloy in relation to sample thickness is shown in Fig. 16. Basing on the literature [12-14], the intensity of $\Delta\mu/\mu$ is directly proportional to the concentration of the defects in amorphous materials, i.e. free volume concentration.

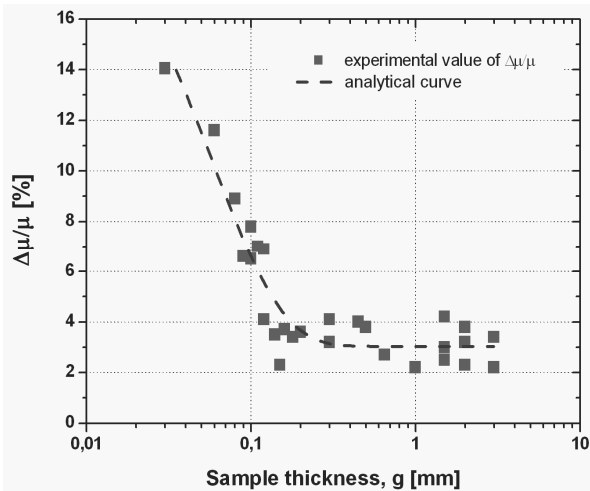


Fig. 16. Magnetic permeability relaxation of $\text{Fe}_{43}\text{Co}_{14}\text{Ni}_{14}\text{B}_{20}\text{Si}_5\text{Nb}_4$ alloy versus sample thickness

The magnetic permeability relaxation ($\Delta\mu/\mu$), which was determined for samples in form of ring, plate and rod had a value of 3.8, 2.2 and 2.2 %, adequately. Finally, Table 2 summarises information concerning magnetic properties of the studied alloy in form of the ring, plate and rod in as-cast state.

The values of coercivity and magnetic permeability might suggest some degree of magnetic inhomogeneity.

Table 2.

Magnetic properties of the studied $\text{Fe}_{43}\text{Co}_{14}\text{Ni}_{14}\text{B}_{20}\text{Si}_5\text{Nb}_4$ samples in forms of ring, plate and rod, in as-cast state

Sample	Thickness [mm]	H_c [A/m]	μ_r	$\Delta\mu/\mu$ [%]
ring	0.5	19	1006	3.8
plate	1	41	879	2.2
rod	3	78	147	2.2

4. Conclusions

The investigations performed on the $\text{Fe}_{43}\text{Co}_{14}\text{Ni}_{14}\text{B}_{20}\text{Si}_5\text{Nb}_4$ bulk metallic glass in form of rings, plates and rods allowed to formulate the following statements:

- the XRD and TEM investigations revealed that the studied as-cast bulk glassy samples were amorphous,
- the SEM images showed that studied fractures of ring, plate and rod in as-cast state indicated two structurally different zones,
- changes of crystallization temperature and glass transition temperature versus the thickness of the glassy samples were stated,
- the supercooled liquid region (ΔT_x) defined by the difference between T_g and T_x , is as large as 56 K for the rod with diameter of 3 mm,
- the initial magnetic permeability decreased but the coercive force increased with increasing sample thickness,
- the magnetic permeability relaxation, which is directly proportional to the microvoids concentration in amorphous structure decreased with increasing sample thickness,
- differences in coercivity and magnetic permeability between samples with different thickness might be resulted by some difference of amorphous structure.

Acknowledgements

The authors would like to thank Dr W. Głuchowski (Non-Ferrous Metals Institute, Gliwice), Dr T. Czeppe (Institute of Metallurgy and Materials Science) and Dr Z. Stokłosa (Institute of Materials Science, University of Silesia, Katowice) for a cooperation and helpful comments.

References

- [1] A. Inoue, K. Hashimoto, Amorphous and nanocrystalline materials: preparation, properties and applications, Springer, 2001.
- [2] A. Inoue, A. Makino, T. Mizushima, Ferromagnetic bulk glassy alloys, Journal of Magnetism and Magnetic Materials 215-216 (2000) 246-252.
- [3] R.B. Schwarz, T.D. Shen, U. Harms, T. Lillo, Soft ferromagnetism in amorphous and nanocrystalline alloys, Journal of Magnetism and Magnetic Materials 283 (2004) 223-230.

- [4] W.H. Wang, C. Dong, C.H. Shek, Bulk metallic glasses, *Materials Science and Engineering R* 44 (2004) 45-89.
- [5] A. Inoue, B. Shen, A. Takeuchi, Fabrication, properties and applications of bulk glassy alloys in late transition metal-based systems, *Materials Science and Engineering A* 441 (2006) 18-25.
- [6] R. Nowosielski, R. Babilas, Structure and magnetic properties of $\text{Fe}_{36}\text{Co}_{36}\text{B}_{19}\text{Si}_5\text{Nb}_4$ bulk metallic glasses, *Journal of Achievements in Materials and Manufacturing Engineering* 30/2 (2008) 135-140.
- [7] R. Nowosielski, R. Babilas, Structure and properties of selected Fe-based metallic glasses, *Journal of Achievements in Materials and Manufacturing Engineering* 37/2 (2009) 332-339.
- [8] R. Nowosielski, R. Babilas, Fabrication of bulk metallic glasses by centrifugal casting method, *Journal of Achievements in Materials and Manufacturing Engineering* 20 (2007) 487-490.
- [9] D. Szewieczek, T. Raszka, Structure and magnetic properties of $\text{Fe}_{63.5}\text{Co}_{10}\text{Cu}_1\text{Nb}_3\text{Si}_{13.5}\text{B}_9$ alloy, *Journal of Achievements in Materials and Manufacturing Engineering* 19 (2006) 179-182.
- [10] D. Szewieczek, T. Raszka, J. Olszewski, Optimisation the magnetic properties of the $(\text{Fe}_{1-x}\text{Co}_x)_{73.5}\text{Cu}_1\text{Nb}_3\text{Si}_{13.5}\text{B}_9$ ($x=10; 30; 40$) alloys, *Journal of Achievements in Materials and Manufacturing Engineering* 20 (2007) 31-36.
- [11] S. Lesz, D. Szewieczek, J.E. Frąckowiak, Structure and magnetic properties of amorphous and nanocrystalline $\text{Fe}_{85.4}\text{Hf}_{1.4}\text{B}_{13.2}$ alloy, *Journal of Achievements in Materials and Manufacturing Engineering* 19 (2006) 29-34.
- [12] P. Kwapuliński, J. Rasek, Z. Stokłosa, G. Badura, B. Kostrubiec, G. Haneczok, Magnetic and mechanical properties in FeXSIB ($X=\text{Cu, Zr, Co}$) amorphous alloys, *Archives of Materials Science and Engineering* 31/1 (2008) 25-28.
- [13] G. Badura, J. Rasek, Z. Stokłosa, P. Kwapuliński, G. Haneczok, J. Lelaćko, L. Pająk, Soft magnetic properties enhancement effect and crystallization processes in $\text{Fe}_{78-x}\text{Nb}_x\text{Si}_{13}\text{B}_9$ ($x = 0, 2, 4$) amorphous alloys, *Journal of Alloys and Compounds* 436 (2007) 43-50.
- [14] P. Kwapuliński, Z. Stokłosa, J. Rasek, G. Badura, G. Haneczok, L. Pająk, L. Lelaćko, Influence of alloying additions and annealing time on magnetic properties in amorphous alloys based on iron, *Journal of Magnetism and Magnetic Materials* 320 (2008) 778-782.
- [15] A. Inoue, B.L. Shen, C.T. Chang, Fe- and Co-based bulk glassy alloys with ultrahigh strength of over 4000 MPa, *Intermetallics* 14 (2006) 936-944.